Low-Haze Irregular Nanostructures Fabricated via a Simple Process for Uniform Internal Light Extraction Film in OLEDs

***Geun Su Choi*[1,2], *Eun Jeong Bae*[1,2], *Young Hwan Yu*[2], *Byeong-Kwon Ju*[1,*], *and Young Wook Park*[2,*]**

[1]Display and Nanosensor Laboratory, Department of Electrical Engineering, Korea University, 145, Anam-ro, Seongbuk-gu, Seoul 02841, Republic of Korea.

[2]Nano and Organic-Electronics Laboratory, Department of Display and Semiconductor Engineering, Sun Moon University, Asan 31460, Republic of Korea

Contact Author's E-mail : bkju@korea.ac.kr[1,*], zerook@sunmoon.ac.kr[2,*]

Abstract

Low-haze light extraction from OLEDs was achieved using nanoscale corrugation fabricated via plasma treatment. The irregular nanostructure (INS) showed 1.6% haze, comparable to bare glass, with 10% angular-integrated intensity enhancement. Modulating refractive index by gas type and treatment time enables application to broad-spectrum, flexible OLED displays.

Author Keywords

OLEDs; irregular nanostructure; internal light-extraction; light out-coupling; mask-free process;

1. Objective and Background

Organic light-emitting diodes (OLEDs) technology has driven significant advancements in display and lighting applications, but internal light loss continues to limit external light extraction efficiency. [1-3] External light extraction methods, typically applied to the substrate's exterior, often utilize micro/nano-structured approaches. [4] Among these, micro-lens arrays (MLA) are widely employed to enhance light extraction. [5] However, their efficiency decreases with smaller lens arrays sizes, and their limited viewing angles and rigid substrate compatibility present challenges. [6] In contrast, internal light extraction techniques, such as those targeting waveguide modes, have the potential to maximize light extraction efficiency by addressing light trapped within the device. [7] Despite their promise, these methods face significant barriers due to complex fabrication processes and technical challenges, hindering widespread adoption.

This study proposes a simple, low-temperature, and mask-free method to fabricate irregular nanostructure designed to enhance both internal and external light extraction in OLEDs. The investigation focuses on the influence of structural parameters, such as overall density and individual nanostructure dimensions, on light extraction efficiency. The findings aim to offer practical design insights to mitigate light loss in both internal and external regions of OLEDs.

2. Experimental

To enhance the light extraction efficiency of OLEDs, a scattering layer with irregular nanostructures was fabricated using a plasma treatment process. The experiment began with the preparation of a clean glass substrate, selected for its optical transparency and compatibility with the fabrication process. Subsequently, a negative photoresist, such as SU-8, was spin-coated onto the glass substrate to form a uniform and well-controlled layer. The thickness of the photoresist layer was carefully adjusted, as it directly influenced the height and density of the resulting nanostructures. After spin coating, the photoresist layer was pre-baked on a hotplate to stabilize the coating. The photoresist-coated substrate was subjected to plasma treatment to create irregular nanostructures. (Fig. 1) To control the morphology and density of the nanostructures, plasma treatment was performed using single gases, including Ar, CHF_3, and CF_4. Single-gas plasma treatment offers the advantage of precise structural modulation while avoiding the complexity associated with mixed-gas environments. The fabricated nanostructures were characterized using scanning electron microscopy (SEM) to confirm their formation and evaluate their morphological properties. SEM imaging revealed the distribution, height, and density of the nanostructures, which were further optimized by adjusting the plasma treatment parameters. To evaluate the impact of the irregular nanostructure film on OLED characteristics, it was applied to a commercial white OLED panel. This integration allowed for the investigation of angular dependencies in radiant intensity.

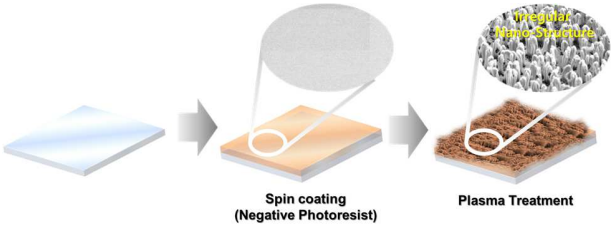

Figure 1. Schematic of the irregular nanostructure light-extraction film fabrication process.

3. Results

The SEM images reveal the morphological differences in nanostructures formed under plasma treatments with Ar, CHF_3, and CF_4 gases. Plasma treatment with Ar gas produced sparse nanostructures with low height, while CHF_3 gas resulted in denser nanostructures with similarly low height. In contrast, CF_4 gas yielded densely packed, high-aspect-ratio pillar nanostructures. These results demonstrate the critical influence of gas type on the height and density of the fabricated nanostructures. (fig 2)

The bare/MLA sample showed consistently low total transmittance of around 40%, indicating significant light scattering or absorption due to its structural characteristics. In contrast, the bare/non-patterned SU-8 sample exhibited high transmittance above 80%, as the absence of structural patterns allowed light to pass with minimal interference.

ISSN 0097-996X/25/5603-2307-$1.00 © 2025

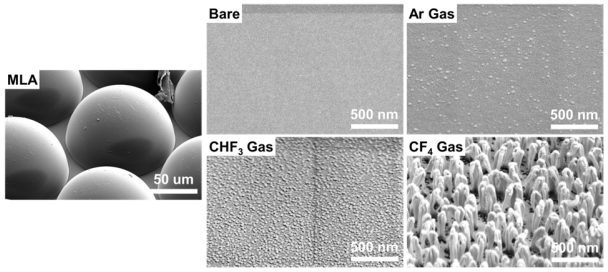

Figure 2. SEM images of nanostructures fabricated on 75 μm hemisphere MLA and non-patterned SU-8 surfaces using single-gas plasma treatments for 8 minutes.

For plasma-treated samples, transmittance varied by gas type. Ar-treated samples had slightly lower transmittance than the bare/non-patterned photoresist SU-8 sample, with a gradual decline as treatment duration increased, due to the formation of low-density nanostructures. CHF_3-treated samples showed further reductions in transmittance, linked to higher-density nanostructures. CF_4-treated samples exhibited the highest transmittance, attributed to densely packed, high-aspect-ratio nanostructures that strongly scattered light. The bare/MLA sample exhibited haze values exceeding 80% across all wavelengths, reflecting strong light scattering. In contrast, the bare/non-patterned SU-8 sample had haze values below 0.8%, indicating negligible scattering due to its smooth surface. For plasma-treated samples, haze increased with nanostructure density and aspect ratio. Ar-treated samples had slightly higher haze than bare/non-patterned SU-8, while CHF_3-treated samples showed further increases with treatment duration. CF_4-treated samples demonstrated the highest haze, driven by densely packed, high-aspect-ratio nanostructures. The bare/non-patterned PR sample showed the highest transmittance and lowest haze due to minimal light scattering. Plasma-treated samples exhibited reduced transmittance and increased haze in the order of Ar < CHF_3 < CF_4, reflecting the influence of nanostructure density and aspect ratio. CF_4-treated samples, with the strongest scattering properties, hold potential for enhanced light extraction applications. (fig 3)

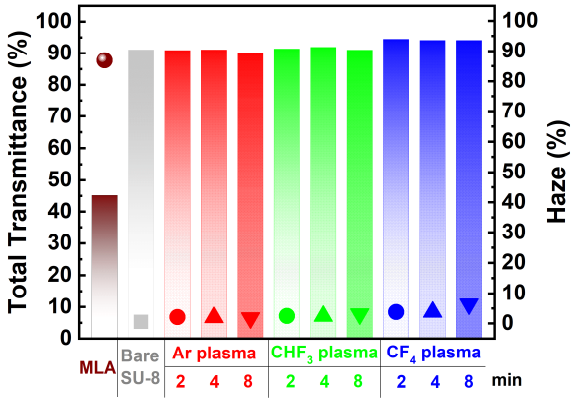

Figure 3. Total transmittance (bars) and haze (solid symbols) of SU-8 and MLA films formed on soda-lime glass at a wavelength of 550 nm. The red, green, and blue represent SU-8 films treated with Ar, CHF_3, and CF_4 plasma, respectively, for different treatment times.

Fig 4 presents the angular distribution of normalized luminance for various samples, emphasizing the differences in light-scattering properties and luminance uniformity across viewing angles. The integrated area under each curve provides a quantitative measure of the luminance distribution. The MLA sample exhibits the smallest integrated area among all samples, indicating that, although significant light scattering occurs, the overall luminance intensity is low. This suggests that the MLA structure effectively redistributes light across a wide range of angles but at the cost of reducing the total luminance. In contrast, the Bare sample demonstrates a larger integrated area than the MLA, as most light is concentrated around 0°, resulting in a steep decline in luminance with increasing viewing angle. This highlights the limited light-scattering properties of the Bare surface. The Non-patterned SU-8 sample shows a slightly larger integrated area than the bare sample, suggesting that the smooth surface minimally influences light distribution but allows for slightly better angular luminance uniformity. However, the overall light-scattering effect remains low. Among the plasma-treated samples, the integrated area increases with the density and height of the nanostructures formed during the plasma process. The Ar gas-treated sample exhibits a moderate integrated area, reflecting the presence of low-density nanostructures that provide a slight improvement in angular luminance uniformity. The CHF_3-treated sample shows a further increase in the integrated area, attributed to higher-density nanostructures that enhance light scattering more effectively. The CF_4-treated sample achieves the largest integrated area, which corresponds to densely packed, high-aspect-ratio nanostructures that distribute luminance more uniformly across a wide range of viewing angles. The MLA sample redistributes light effectively but suffers from low total luminance, while the plasma-treated samples, particularly those treated with CF_4 gas, demonstrate the best balance between luminance intensity and angular distribution. These results highlight the potential of CF_4-treated nanostructures for applications requiring improved light extraction and uniform luminance distribution over wide viewing angles.

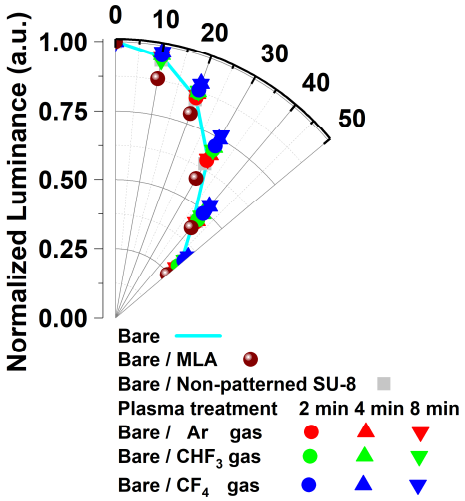

Figure 4. Comparison of normalized luminance as a function of viewing angle for different samples, including Bare, MLA, Non-patterned SU-8, and plasma-treated samples with Ar, CHF_3, and CF_4 gases.

The bare/non-patterned SU-8 sample exhibited a consistent refractive index of n=1.90 across all measured wavelengths. This uniformity reflects the unaltered optical properties of the untreated surface. The Ar gas-treated samples showed a slightly reduced average refractive index of n=1.95, with values ranging from n=1.92 to 1.96 depending on the treatment duration. This suggests that the low-density nanostructures formed during Ar plasma treatment marginally affected the light path, leading to a moderate reduction in n. The CHF_3 gas-treated samples demonstrated a further decrease in refractive index, with an average value of n=1.93 and a range of n=1.91 to 1.94. This reduction is attributed to higher-density nanostructures that more significantly influenced the light path. The CF_4 gas-treated samples exhibited the most pronounced changes, with an average refractive index of n=1.85 and a range of n=1.81 to 1.88. These values reflect the densely packed, high-aspect-ratio nanostructures formed during CF_4 plasma treatment, which had the greatest impact on light scattering and refractive behavior. The extinction coefficient (k) showed a general decrease across all samples as the wavelength increased, indicating relatively low light absorption within the visible range. Notably, the CF_4-treated samples exhibited the lowest extinction coefficients, emphasizing the dominance of scattering effects over absorption in these structures. These results suggest that the modulation of the refractive index, driven by plasma treatment parameters such as gas type and duration, significantly contributed to the observed changes in the integrated luminance area. Specifically, the CF_4 gas-treated samples, with their highly modulated refractive index, demonstrated the most uniform luminance distribution and enhanced light extraction. This highlights the potential of CF_4-treated nanostructures for applications requiring improved optical efficiency and angular light uniformity.

4. Impact

This study demonstrates the successful fabrication of low-haze irregular nanostructures (IRN) using a simple plasma treatment process. The CF_4-treated samples, characterized by densely packed, high-aspect-ratio nanostructures, achieved a haze of 1.6% and a 10% enhancement in angular-integrated luminance, demonstrating superior light extraction efficiency. In comparison to MLA, the IRN structures showed a more uniform angular light distribution while maintaining high optical efficiency. While MLA exhibited strong light-scattering properties, its overall luminance was lower, highlighting its limitations in achieving balanced optical performance. Plasma treatment parameters, such as gas type and duration, played a critical role in modulating the refractive index and extinction coefficient of the nanostructures, significantly influencing their light extraction capabilities. The CF_4-treated samples, in particular, exhibited the lowest extinction coefficient and the most uniform luminance distribution across wide viewing angles, making them ideal for flexible OLED applications. These findings underscore the potential of IRN structures in addressing the limitations of traditional MLA-based approaches. The proposed method offers a scalable and efficient solution for enhancing light extraction and angular luminance uniformity, paving the way for high-performance, flexible OLED displays.

5. Acknowledgements

This work was supported by the National Research Foundation of Korea (NRF-2020R1C1C1013567) grant funded by the Korea government (MSIT) and was supported by "Regional Innovation Strategy (RIS)" through the National Research Foundation of Korea (NRF) funded by the Ministry of Education (MOE)(2021RIS-004), and we thank the Center for Next Generation Semiconductor Technology at SUNMOON University for analysis support.

6. References

[1] Lee, S., Park, J. Y., Park, J., Bi, J. C., Kang, B., Hwang, Y. H., ... & Ju, B. K., Advanced Electronic Materials, 2023, 9, 2201264.

[2] Do, Y. R., Kim, Y. C., Song, Y. W., & Lee, Y. H., Journal of Applied Physics, 2004, 96, 7629-7636.

[3] Bae, H., Kim, J. S., & Hong, C., Optics Communications, 2018, 415, 168-176.

[4] Bae, E. J., Kang, S. W., Choi, G. S., Jang, E. B., Baek, D. H., Ju, B. K., & Park, Y. W. (2022). Enhanced light extraction from organic light-emitting diodes with micro-nano hybrid structure. Nanomaterials, 12(8), 1266.

[5] Qu, Y., Kim, J., Coburn, C., & Forrest, S. R. (2018). Efficient, nonintrusive outcoupling in organic light emitting devices using embedded microlens arrays. ACS photonics, 5(6), 2453-2458.

[6] Salehi, A., Fu, X., Shin, D. H., & So, F. (2019). Recent advances in OLED optical design. Advanced Functional Materials, 29(15), 1808803.

[7] Lee, K., Shin, J. W., Park, J. H., Lee, J., Joo, C. W., Lee, J. I., D. H., Cho, J. T., Lim, M. C., Oh, Ju, B. K., & Moon, J. (2016). A light scattering layer for internal light extraction of organic light-emitting diodes based on silver nanowires. ACS applied materials & interfaces, 8(27), 17409-17415.